

Dynamical LEED study of Pt(111)-($\sqrt{3} \times \sqrt{3}$)R30°-Xe

Th. Seyller, M. Caragiu, and R. D. Diehl*

Physics Department, Penn State University, University Park, Pennsylvania 16802

P. Kaukasoina and M. Lindroos

Physics Department, Tampere University of Technology, 33101 Tampere, Finland

(Received 3 February 1999; revised manuscript received 27 April 1999)

Low-energy electron diffraction (LEED) studies of Pt(111)-($\sqrt{3} \times \sqrt{3}$)R30°-Xe at 80 K and 110 K indicate that the Xe adsorption site is on top of the Pt atoms with a Xe-Pt distance of 3.4 Å. The substrate structure is essentially unrelaxed with respect to the bulk. These results contrast with an earlier spin-polarized LEED study which indicated that hollow sites are occupied in this structure. The low-coordination-site geometry for Xe is discussed in the context of earlier studies of Xe adsorption. [S0163-1829(99)03939-9]

INTRODUCTION

The adsorption site of Xe on Pt(111) has been a point of study and conjecture since the extraordinary proposal was made in 1990 that Xe might occupy the low-coordination top sites instead of the high-coordination hollow sites.¹ This proposal was based on the analysis of He-atom diffraction data from the low-temperature ($T < 60$ K) uniaxially compressed phase of Xe on Pt(111).^{2,3} The diffraction intensities from this incommensurate domain-wall structure were shown to be consistent with a triangular array of adsorption sites, such as would be found for an array of top sites as shown in Fig. 1(a). The array produced by the hollow sites has a honeycomb symmetry, as shown in Fig. 1(b), which was deemed to be inconsistent with the He diffraction results. It was pointed out that if the adsorption energies for Xe in the hcp hollow and the fcc hollow sites are significantly different, then Xe might occupy just one type of hollow site, also leading to a triangular array.^{1,4} However, little if any adsorption energy difference was expected for the two types of hollow sites, and therefore top-site occupation by Xe atoms was proposed.

This rather shocking proposal was supported by a density-functional theory calculation for Xe adsorbed on a Pt cluster.⁵ This calculation indicated that the top site was preferred over the hollow sites by about 30 meV. This calculation cannot be considered to be complete since the van der Waals interaction was not included. However, its interpretation suggested that a top-site preference might arise from a hybridization of the Xe $5p$ states with the unoccupied $5d$ states near the Fermi level in the Pt surface.⁵ Additional support for the top-site geometry was provided by a recent study of the phonons of the commensurate ($\sqrt{3} \times \sqrt{3}$)R30° structure.⁶ In that study, a comparison of the magnitude of the energy gap for the in-plane Xe vibrations at the zone center to model calculations strongly suggested that the experimental data were consistent with the top-site model.⁶

While the indirect evidence of top-site preference of Xe on Pt(111) has been mounting, a direct measurement of the site would be more convincing. Such a measurement was made using spin-polarized low-energy electron diffraction (SPLEED) to study the commensurate ($\sqrt{3} \times \sqrt{3}$)R30° structure in 1995.⁷ The result indicated that Xe adsorbs preferen-

tially in hollow sites, with equal occupations of fcc and hcp sites, which together form a honeycomb array of sites. This result therefore disagrees with the He-atom scattering studies discussed above. Since SPLEED determines the actual adsorption site rather than the symmetry of adsorption sites and does not require a model of the potential energy surface for its interpretation, it is the more direct approach to determining the adsorption site. However, the Xe-Pt interlayer distance determined from the SPLEED study was 4.2 ± 0.1 Å, which is exceedingly long compared to the corresponding hard-sphere interlayer spacing for hollow-site adsorption of 3.2 Å (see Table I). Nevertheless, this hollow-site result was bolstered by a similar SPLEED study of the same structure of Xe on Pd(111), which also indicated hollow-site adsorption.⁸ Interestingly, however, a SPLEED study of the lower-coverage disordered phase of Xe on Pd(111) indicated top-site occupation of the Xe atoms.⁸ This result was deemed to be consistent with the cluster calculation for Xe/Pt(111), which most closely resembled a low coverage of Xe. Thus, the picture which emerged from these SPLEED studies is that Xe prefers the top sites at low coverages, but hollow sites at higher coverages. The mechanism for this change in site preference was proposed to be the Xe depolarization and the concomitant weakening of the Xe-Pt chemical bond which occurs at higher coverages due to the increased Xe-Xe interactions.

More recently, however, Xe has been determined by low-energy electron diffraction (LEED) studies to occupy top sites in the ($\sqrt{3} \times \sqrt{3}$)R30° structure on other metal surfaces, namely Ru(0001) (Ref. 9) and Cu(111).¹⁰ These results do not fit the picture described above, unless the Xe atoms are

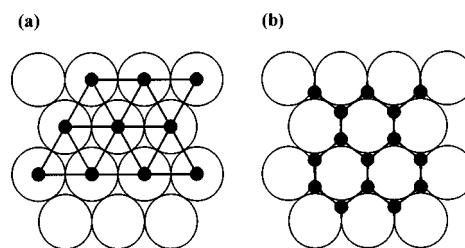


FIG. 1. fcc(111) surface showing the arrays of adsorption sites if (a) the top site is preferred and (b) if hollow sites are preferred.

TABLE I. Gas-substrate sites and interlayer spacings (in Å) determined for Xe on various metal surfaces. The “hard-sphere” model predictions are calculated using nearest-neighbor spacings found in solids. q is the monolayer adsorption energy in meV (Refs. 20 and 21). Italics indicate earlier results that we now believe are inaccurate.

System	Site	Gas-substrate interlayer spacing	Hard-sphere interlayer spacing	q
Cu(111)-($\sqrt{3}\times\sqrt{3}$)R30°-Xe (Ref. 10)	top	3.60 ± 0.08	3.47	200 (Refs. 20, 21) ^a
Ru(0001)-($\sqrt{3}\times\sqrt{3}$)R30°-Xe (Ref. 9)	top	3.54 ± 0.06	3.54	230 (Ref. 22)
<i>Pt(111)-($\sqrt{3}\times\sqrt{3}$)R30°-Xe (Ref. 7)</i>	<i>hcp/fcc</i>	4.2 ± 0.1	3.20	320 (Ref. 20)
Pt(111)-($\sqrt{3}\times\sqrt{3}$)R30°-Xe	top	3.4 ± 0.1	3.58	320 (Ref. 20)
<i>Pd(111)-($\sqrt{3}\times\sqrt{3}$)R30°-Xe (Ref. 8)</i>	<i>hcp/fcc</i>	3.5 ± 0.1	3.20	330 (Ref. 23)
Pd(111)-($\sqrt{3}\times\sqrt{3}$)R30°-Xe (Ref. 15)	top	^b	3.56	330 (Ref. 23)
Pd(111)-disordered-Xe (Ref. 8)	top	4.0 ± 0.1	3.56	360 ^c (Ref. 23)

^aEstimated value based on values published for similar surfaces.

^bAnalysis incomplete.

^cInitial adsorption energy.

more strongly polarized on Ru and Cu than on Pt and Pd. In fact, the heats of adsorption for Xe are smaller for Cu and Ru (see Table I) suggesting a smaller polarization in these cases. The weakest possible adsorption bonds are ones with no hybridization, and with no hybridization the hollow sites will surely be preferred. Therefore it seems paradoxical that in the cases we know of, the most strongly bound Xe atoms appear to be in the hollow sites and the most weakly bound ones are in top sites.

EXPERIMENTAL AND CALCULATIONAL PROCEDURES

In order to obtain more information to help to resolve this conundrum, we undertook a LEED study of the ($\sqrt{3}\times\sqrt{3}$)R30° structure of Xe on Pt(111). The experiments were performed at 80 K and 110 K using a low-current video LEED system described in detail elsewhere.¹¹ The Pt(111) crystal was cleaned by successive cycles of Ar⁺ ion bombardment and annealing at 700 °C until no impurities could be observed in the Auger-electron spectrum. Xe was adsorbed at a temperature of 100 K by backfilling the chamber with Xe. The adsorbed Xe formed a well-ordered ($\sqrt{3}$

$\times\sqrt{3}$)R30° structure as seen by sharp superlattice spots. To stabilize this structure at 110 K, it was necessary to maintain a partial pressure of 2×10^{-7} mbar of Xe.

A LEED pattern from the Pt(111)-($\sqrt{3}\times\sqrt{3}$)R30°-Xe structure is shown in Fig. 2. To analyze the LEED intensity data, the initial searches through different adsorption sites were done using the Barbieri–Van Hove symmetrized automated tensor LEED (SATLEED) package.¹² The phase shifts were calculated with the Barbieri–Van Hove phase-shift program¹² using muffin-tin radii equal to the touching radius of the atoms. We tested adsorption in top, fcc, and hcp hollow sites and a mixture of the two different hollow sites. Theoretical and experimental $I(E)$ spectra were compared using the Pendry R factor.¹³ Figures 3(a) and 3(b) show the experimental and best-fit calculated spectra for the 80 and 110 K datasets, respectively. Table II summarizes the optimum Pendry R factors (R_p) for the different structural models tested in our analysis. R_{fr} is the optimum Pendry R factor for the fractional-order beams only. From these results we can rule out other models in favor of the on-top adsorption. To see what these R factors mean in terms of agreement, Fig. 4 compares a fractional-order experimental curves to the calculated curves for the top-site model and for the mixed-

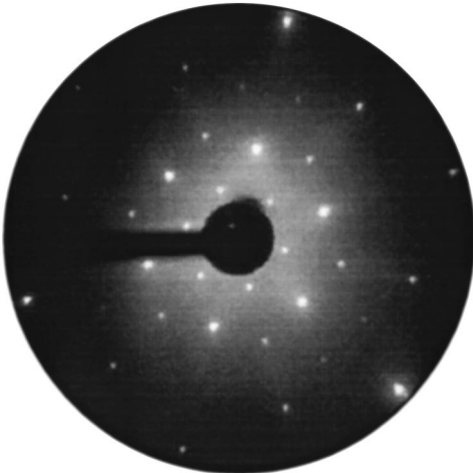


FIG. 2. LEED pattern from Xe on Pt(111) at $T=110$ K, $p=2\times 10^{-7}$ mbar, and $E=290$ eV. The inner ring of spots corresponds to first-order overlayer diffraction of the ($\sqrt{3}\times\sqrt{3}$)R30° structure.

TABLE II. Optimum Pendry R factors for different structural models tested with SATLEED (Ref. 12), for the two datasets. R_p is the overall R factor for each geometry and R_{fr} is the best R factor for the fractional-order beams only.

$T=80$ K	R_p	R_{fr}
hcp hollows	0.52	0.72
fcc hollows	0.58	0.85
top	0.34	0.39
60% hcp+40% fcc	0.48	0.70
$T=110$ K	R_p	R_{fr}
hcp hollows	0.46	0.70
fcc hollows	0.47	0.72
top	0.30	0.41
60% hcp+40% fcc	0.41	0.62

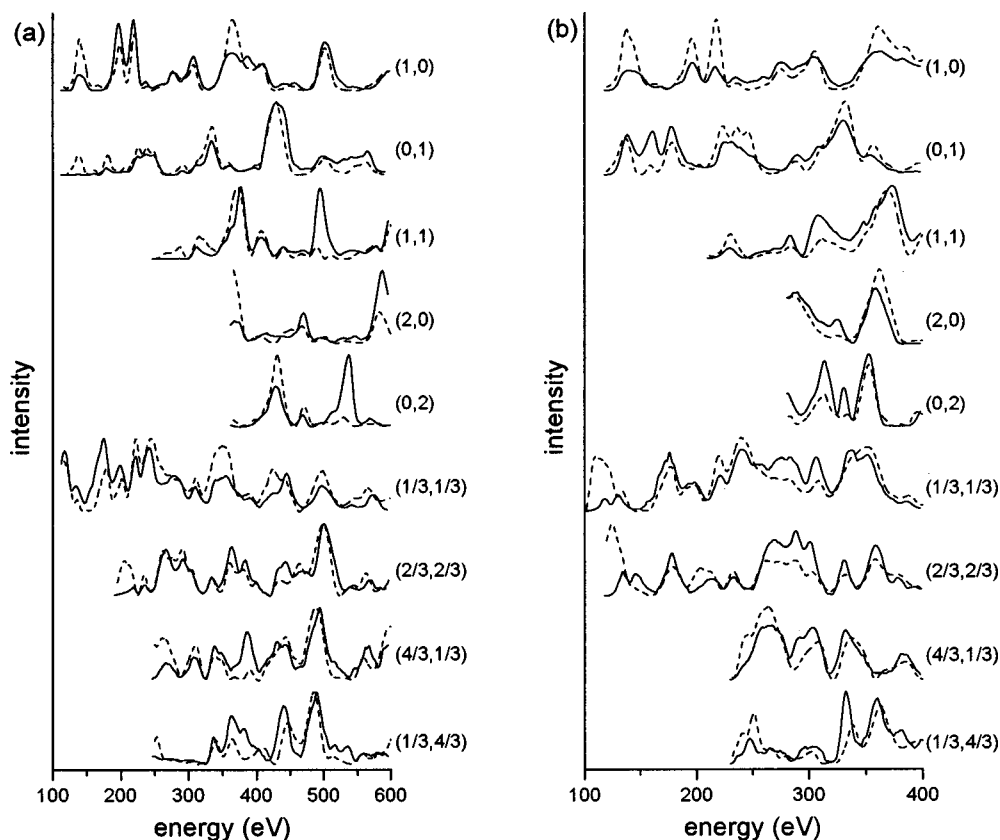


FIG. 3. Best-fit theoretical and experimental $I(E)$ spectra for top-site adsorption of Xe on Pt(111) for (a) 80 K and (b) 110 K. The solid curves are from the experiment and the dashed curves are calculated.

hollow-site model. While peaks at some energies are present in both calculated spectra, there are considerably more features in the calculated top-site spectra that match the experimental spectra.

The refinement of the top-site structure, including vibrations, was carried out using the LEED package of Van Hove and Tong.¹⁴ In these calculations, 11 phase shifts were used in the scattering from Pt and 21 in the scattering from Xe. The imaginary part of the inner potential was taken to be proportional to the cubic root of the electron energy, being -4.6 eV at an electron energy of 90 eV. The real part of the inner potential was varied in the R -factor analysis in steps of 0.2 eV and the final value was 7.5 eV for the 110 K dataset and 5.3 eV for the 80 K dataset. A Debye temperature of 200 K was used for the first Pt layer and 280 K for the other layers. The Xe vibrations were allowed to be anisotropic using a method described elsewhere.¹⁴ The total energy ranges of nine symmetrically inequivalent beams in the experimental spectra was about 1900 eV for the 110 K dataset and 3400 eV for the 80 K dataset.

RESULTS AND DISCUSSION

Although there is a very clear preference for the top-site geometry, the determination of the adsorption distance of the Xe was hindered by the insensitivity of the calculated spectra to the Xe-Pt distance. This insensitivity is at least partially a result of the relatively large perpendicular Xe vibrational amplitude which reduces the backscattered amplitude from the Xe atoms. The calculated spectra were more sensitive to the

Xe-Pt distance if the vibration amplitude parameters were kept small in the calculation; however, the overall level of agreement was much better for the larger amplitudes. The result of this insensitivity to $d_{\text{Xe-Pt}}$ is that the precision of this parameter is quite poor in this structural analysis; nevertheless, the sensitivity to the other structural parameters is not so much affected. Figure 5 shows the variation in the Pendry R factor with the Xe-Pt distance after other parameters had been optimized for each dataset. These curves show oscillations in the R factors, which are expected since they reflect the constructive and destructive interference conditions

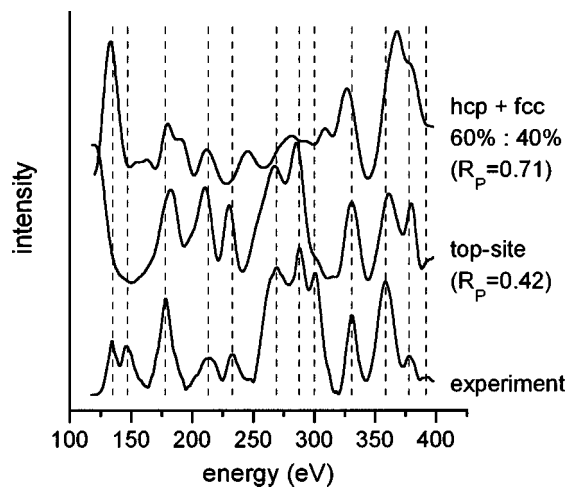


FIG. 4. A comparison of the experimental and calculated $(2/3, 2/3)$ beams for the top-site and mixed-hollow-site structures.

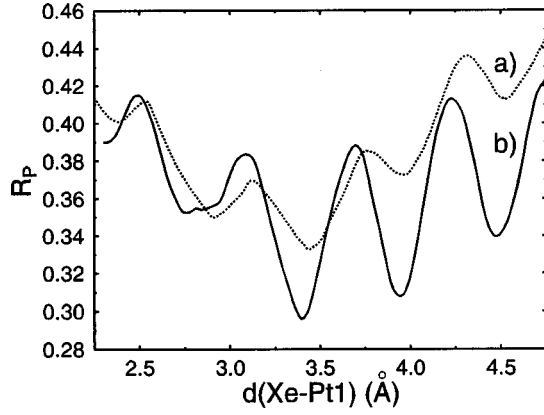


FIG. 5. Variation in the Pendry R factor as a function of the Xe-Pt spacing after all other parameters have been optimized for the 3.4-Å minimum for the (a) 80 K dataset, and (b) 110 K dataset.

which occur as the wavelength (or energy) is scanned. However, the maxima between the local minima are unusually shallow in these cases, and there is very little difference between the two lowest minima in both cases, making them almost indistinguishable. For the 80 K dataset, the two lowest minima occur at about 2.9 and 3.4 Å, while for the 110 K dataset, the two lowest minima occur at about 3.4 and 3.9 Å.

While by inspection and by R -factor analysis it is not possible to distinguish between the two lowest minima in each case, we note that the minimum at 3.4 Å is lowest in both cases, and this distance is also closest to the hard-sphere distance for Xe-Pt, 3.58 Å. Therefore we have assumed that this is the correct minimum and have optimized all other parameters for this minimum. The resulting structural parameters for the two datasets are given in Table III. These results indicate that the structural parameters are essentially identical for the two temperatures, with the exception of the parallel vibration amplitude, which is about 50% larger for the higher temperature. For $T \gg \Theta_D$, which is the case we have here ($T \geq 80$ K and $\Theta_D = 55$ K), the mean-square vibrations in a normal harmonic solid should increase linearly with temperature.¹⁴ Using the relationship

$$\langle \Delta r^2 \rangle = (2\langle \Delta r_{\text{par}}^2 \rangle + \langle \Delta r_{\text{perp}}^2 \rangle) / 3$$

and using the values given in Table III, the mean square vibration amplitude for the 110 K case is about twice that of

the 80 K case, which is considerably larger than the ratio of the temperatures, $110/80=1.4$. The large errors on the experimentally determined vibration amplitudes preclude a quantitative analysis, but their faster-than-linear increase is consistent with anharmonic behavior, which should be expected close to the monolayer melting temperature, which is near 110 K for these experimental conditions.²

The most important aspect of this structural determination, however, is the adsorption site of Xe. As discussed above, the earlier studies gave a somewhat ambiguous picture of this situation since there was not sufficiently stringent evidence for either the top site or the hollow sites. The present top-site determination is consistent with all other studies except the spin-polarized LEED study, which found hollow sites. It is not clear to us why the spin-polarized LEED study should give a different structural result, but we note that it included an extremely large Xe-Pt interlayer spacing of 4.2 Å, compared to the 3.2 Å expected from a hard-sphere packing model for hollow-site adsorption. We tested the distance 4.2 Å for the model which includes both hcp and fcc sites, and the best agreement we found gave an overall R factor of 0.51 and a fractional-order R factor of 0.72. This is somewhat worse than the values obtained for a smaller spacing for this model (see Table II) and considerably worse than the top-site values. While the result quoted in the spin-polarized LEED study was the global minimum of the reliability factor, a local minimum was also quoted for the top site with an interlayer spacing of 3.6 Å. This value is close to both our results and to the hard-sphere interlayer spacing of 3.58 Å for the top site.

This top-site determination for Xe/Pt(111) and another recent top-site determination for Xe/Pd(111) (Ref. 15) also resolve the ambiguous trend of the adsorption site of Xe vs the adsorption strength (see Table I). Now, top sites have been observed in the ($\sqrt{3}\times\sqrt{3}$)R30° structure for Xe on all four substrates, Cu(111), Pt(111), Pd(111), and Ru(0001). The LEED studies provide no evidence for a site change as a function of adsorption strength. Since the Xe-Xe spacing in this structure on both Pt(111) and Pd(111) (4.76–4.80 Å) is very expanded relative to its usual spacing of about 4.4 Å, it is unlikely that the Xe-Xe interaction plays a large role in this site preference. Indeed, both specular He-atom scattering measurements¹⁶ and the recent inelastic He-atom scattering measurements⁶ for Xe on Pt(111) have indicated that the

TABLE III. Optimum structural parameters for the two R -factor minima. R_p is the Pendry R factor and R_{fr} is the R factor for just the fractional-order beams. δPt1 refers to a rumple in the top layer of Pt in which the Pt atom directly beneath the Xe atom is pushed inward, toward the bulk.

Pt(111)-($\sqrt{3}\times\sqrt{3}$)R30°-Xe	80 K	110 K
$d(\text{Xe-Pt1})$	3.4 ± 0.2 Å	3.4 ± 0.1 Å
δPt1 (rumple)	0.00 ± 0.02 Å	0.01 ± 0.03 Å
$d(\text{Pt1-Pt2})$	2.31 ± 0.02 Å	2.29 ± 0.03 Å
$d(\text{Pt2-Pt3})$	2.25 ± 0.03 Å	2.28 ± 0.04 Å
$d(\text{Pt3-Pt4})$	2.27 ± 0.03 Å	2.27 ± 0.04 Å
parallel rms Xe amplitude	0.4 ± 0.1 Å	0.6 ± 0.1 Å
perpendicular rms Xe amplitude	0.3 ± 0.1 Å	0.3 ± 0.1 Å
R_p	0.33	0.30
R_{fr}	0.41	0.39

Xe-Xe interactions in this phase are consistent with gas-phase interaction potentials.¹ Therefore the top-site adsorption of Xe on close-packed metal surfaces appears to be a common occurrence. This raises a question as to the mechanism which leads to this preference and whether it also pertains to other substrate morphologies and other rare gases. A scanning tunneling microscopy study has indicated that Xe adsorbs on the low-coordination side of surface steps,¹⁷ for instance, suggesting that the low-coordination preference may extend to other substrate morphologies.

A mechanism for top-site preference which was proposed in the earlier LEED studies^{9,10} suggests that the occupied part of the Xe 6s resonance hybridizes with the unoccupied states in the substrate surface, which are localized at the position of the atoms. Within this model, whether the top sites are preferred or not depends on the strength of the hybridization. An alternative explanation is that the site preference arises from the Pauli repulsion which depends on the symmetry of the interacting wave functions of the adatom and the substrate. This mechanism was found to be responsible for the anticorrelation experienced by He atoms which scatter from Rh(110).^{18,19}

CONCLUSION

We have determined the adsorption geometry of Pt(111)-($\sqrt{3} \times \sqrt{3}$)R30°-Xe at 80 K and 110 K. In this struc-

ture, the Xe atoms occupy top sites on the Pt(111) surface and the Xe-Pt distance is $3.4 \pm 0.2 \text{ \AA}$ and $3.4 \pm 0.1 \text{ \AA}$, respectively. There is essentially no rumpling of the substrate and little if any relaxation of the substrate surface layers relative to their bulk spacing. This result is consistent with earlier He-atom scattering studies,^{1,6} which were shown to be consistent with a top-site geometry, but is inconsistent with an earlier SPLEED result which indicated hollow-site adsorption.⁷ We have summarized four different LEED studies that have found top-site adsorption for Xe adsorbed on close-packed metals, and we know of no corroborated studies that indicate preferential hollow-site adsorption for Xe on any metal surface. Therefore the top-site preference of Xe appears to be the rule rather than the exception on close-packed metal surfaces. We have suggested two possible mechanisms that might contribute to the preference for top sites on metal surfaces. However, many more experiments are required for a fuller understanding of this phenomenon.

ACKNOWLEDGMENTS

We would like to thank L. W. Bruch, P. Zeppenfeld, J. F. Annett, D. M. Eigler, M. Scheffler, K. Hermann, and K.-H. Rieder for many enlightening discussions. We also thank U. Linke and R. David at the IGW, Forschungszentrum Jülich for providing the Pt(111) crystal. This work was supported by NSF Grant Nos. DMR-9629715 and DMR-9817977.

*Author to whom correspondence should be addressed. Electronic address: rdd2@psu.edu

¹J. M. Gottlieb, *Phys. Rev. B* **42**, 5377 (1990).

²K. Kern, R. David, P. Zeppenfeld, R. Palmer, and G. Comsa, *Solid State Commun.* **62**, 391 (1987).

³P. Zeppenfeld, K. Kern, R. David, and G. Comsa, *Phys. Rev. B* **38**, 3918 (1988).

⁴P. Zeppenfeld, G. Comsa, and J. A. Barker, *Phys. Rev. B* **46**, 8806 (1992).

⁵J. E. Müller, *Phys. Rev. Lett.* **65**, 3021 (1990).

⁶L. W. Bruch, A. P. Graham, and J. P. Toennies *Mol. Phys.* **95**, 579 (1998).

⁷M. Potthoff, G. Hilgers, N. Müller, U. Heinzmann, L. Hawnert, J. Braun, and G. Borstel, *Surf. Sci.* **322**, 193 (1995).

⁸G. Hilgers, M. Potthoff, N. Müller, and U. Heinzmann, *Surf. Sci.* **322**, 207 (1995).

⁹B. Narloch and D. Menzel, *Chem. Phys. Lett.* **270**, 163 (1997).

¹⁰Th. Seyller, M. Caragiu, R. D. Diehl, P. Kaukasoina, and M. Lindroos, *Chem. Phys. Lett.* **291**, 567 (1998).

¹¹G. S. Leatherman, R. D. Diehl, P. Kaukasoina, and M. Lindroos, *Phys. Rev. B* **53**, 10 254 (1995).

¹²A. Barbieri and M. A. Van Hove (private communication).

¹³J. B. Pendry, *J. Phys. C* **13**, 937 (1980).

¹⁴M. A. Van Hove and S. Y. Tong, *Springer Series in Chemical Physics* (Springer-Verlag, Berlin, 1979).

¹⁵M. Caragiu, Th. Seyller, and R. D. Diehl (unpublished).

¹⁶G. Comsa, B. Poelsema, and K. Kern, in *Helium Scattering from Surfaces*, edited by E. Hulpke (Springer, Berlin, 1992), p. 243.

¹⁷P. Zeppenfeld, S. Horsch, and G. Comsa, *Phys. Rev. Lett.* **73**, 1259 (1994).

¹⁸K. H. Rieder, G. Parschau, and B. Burg, *Phys. Rev. Lett.* **71**, 1059 (1993).

¹⁹M. Petersen, S. Wilke, P. Ruggerone, B. Kohler, and M. Scheffler, *Phys. Rev. Lett.* **76**, 995 (1996).

²⁰L. W. Bruch, M. W. Cole, and E. Zaremba, *Physical Adsorption: Forces and Phenomena* (Oxford University Press, Oxford, 1997).

²¹G. Vidali, G. Ihm, H.-Y. Kim, and M. W. Cole, *Surf. Sci. Rep.* **12**, 133 (1991).

²²H. Schlichting and D. Menzel, *Surf. Sci.* **272**, 27 (1992).

²³K. Wandelt and J. E. Hulse, *J. Chem. Phys.* **80**, 1340 (1984).